Supplementary Material

Photocatalyst with metal-free electron-hole pair double transfer mechanism for pharmaceutical and personal care products degradation

Tiansheng Chen[a], Qianxin Zhang[a], Xiaoshan Zheng[a], Zhijie Xie[a], Yongqin Zeng[a], Ping Chen[ab], Haijin Liu[c], Yang Liu[d], Wenying Lv[a]*, Guoguang Liu[a]*

[a]*School of Environmental Science and Engineering, Guangdong University of Technology, Guangzhou, 510006, China*

[b]*School of Environment, Tsinghua University, Beijing 100084, China*

[c]*School of Environment, Henan Normal University, Key Laboratory for Yellow River and Huaihe River Water Environment and Pollution Control, Xinxiang 453007, China*

[d]*Faculty of Environmental & Biological Engineering, Guangdong University of Petrochemical Technology, Maoming 525000, China*

* **Corresponding Author**: Wenying Lv, Guoguang Liu

E-mail: lvwy612@163.com; liugg615@163.com;

Telephone: +86-20-39322547

Fax: +86-20-39322548

Address: School of Environmental Science and Engineering, Guangdong University of Technology, No. 100 Waihuan Xi Road, Guangzhou Higher Education Mega Center, Guangzhou, P.R China, Post Code: 510006

Table of Contents

Additional Details on Methods

Text S1. Electrochemical measurements

Photoelectrochemical measurements were analyzed using a CHI-660 electrochemical system (Shanghai, China), which was equipped with a conventional three-electrode electrochemical cell. The as-prepared catalysts on ITO served as the working electrode, while a saturated calomel electrode (SCE) and platinum (Pt) wire were employed as the reference electrode and the counter electrode, respectively. A 450 nm LED lamp (3 x 3 W, Shenzhen lamplic co., LTD, China) was used for illumination. The photocurrent was recorded in a 0.1 M sodium sulfate solution (Na_2SO_4).

Text S2. Transformation products identification

The photocatalytic degradation intermediates of ENR were identified by HRLC-MS-MS (Thermo Scientific Ultimate 3000 RSLC and Q Exactive Orbitrap). Separation was accomplished using a Hypersil GOLD C18 (100 x 2.1 mm, 1.9 μm) with column temperature 40 ℃. Elution was performed at a flow rate of 0.3 mL/min with water that contained 0.1 % (v/v) formic acid as eluent A, and methanol as eluent B. Mass spectral analysis was conducted in positive mode.

Text S3. Determination of ENR concentration

The concentration of ENR were determined by an HPLC system HPLC was carried out by a Waters e2968 instrument which outfit a UV detector, and a 4.6 × 250 mm Zorbax Eclipse XDB C18 reverse-phase column (Agilent, USA) at 40 °C. Other conditions of the detection are listed as follow: mobile phase: methanol/Milli-Q water containing 0.2% formic acid (78:22 v/v); flow rates: 1 mL/min; injection volume: 20μL; and determine wavelength: 278 nm.

Table S1. The characterization details of the Mott-Schottky plots.

Potential parameters	
Init E (V)	-1
Final E (V)	-0.2
Incr E (V)	0.001
Amplitude (V)	0.01
Cycles (below 10	5
Quiet time (sec)	2
Bias DC Current	Below 1
Sensitivity (A/V)	Automation

Table S2. BET surface areas of materials.

Sample	BET surface area ($m^2\ g^{-1}$)	Pore volume ($cm^2\ g^{-1}$)	Pore size (nm)
$g\text{-}C_3N_4$	9.09	0.05	21.12
CN3	15.25	0.08	19.87
0.1CCN3	14.80	0.06	16.49
BN	23.36	0.06	9.44

Table S3. Frontier electron densities on atoms of ENR was calculated via using Gaussian 09 program at the B3LYP/6-311 + g (d, p) level.

(number) Atom		FED^2_{HOMO}+ FED^2_{LUMO}	Point charge	(number) Atom		FED^2_{HOMO}+ FED^2_{LUMO}	Point charge
1	C	0.561056	0.236645	18	N	0.331536	-0.470913
2	C	0.353475	-0.080719	19	C	0.002984	-0.077043
3	C	0.171301	-0.257861	20	C	0.000522	-0.201856
4	C	0.022062	0.311741	21	C	0.003470	-0.24548
5	C	0.437277	-0.165586	27	F	0.068178	-0.251128
6	C	0.064631	0.224907	28	N	0.528481	-0.479031
8	C	0.287490	0.385029	29	C	0.004798	-0.153217
10	C	1.059679	0.270456	30	C	0.026412	-0.009355
11	C	0.136015	-0.40379	31	C	0.048020	0.007165
13	C	0.086737	0.424413	33	C	0.005152	-0.134821
14	O	0.056114	-0.402367	35	N	0.073888	-0.404359
15	O	0.040053	-0.324889	42	C	0.003247	-0.120203
17	O	0.251619	-0.401878	43	C	0.010025	-0.308064

Table S4 Compounds (ENR) identified by HPLC–MS-MS during the photocatalytic degradation of ENR under blue LED light irradiation.

Products	Rt(min)	m/z	Probable Structure
ENR	7.79	359	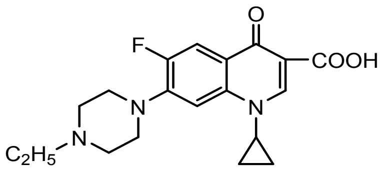
TP1	9.52	265	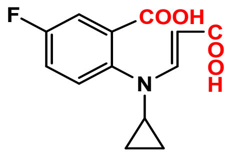
TP2	7.87	357	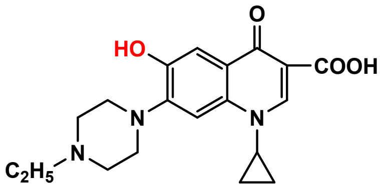
TP3	9.76	389	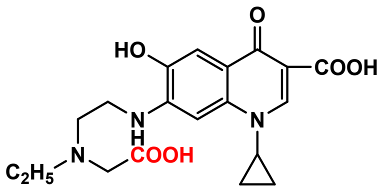
TP4	8.92	361	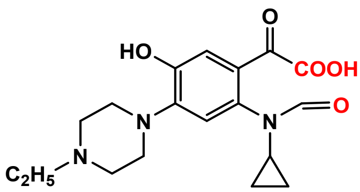
TP5	7.44	375	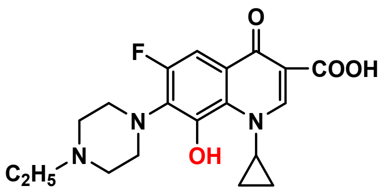
TP6	6.89	373	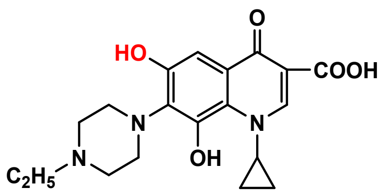
TP7	7.71	331	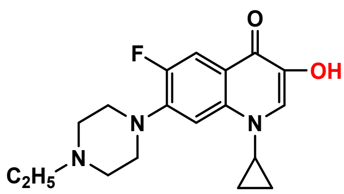

TP8	10.0	333	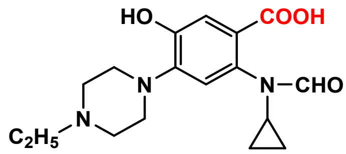

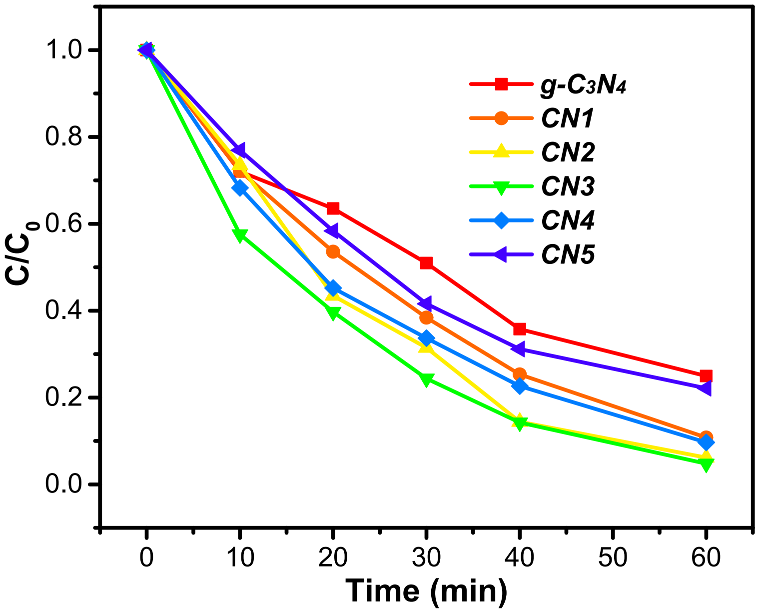

Fig. S1. Photocatalytic degradation of ENR with different photocatalysts (CN-x) under blue LED light irradiation

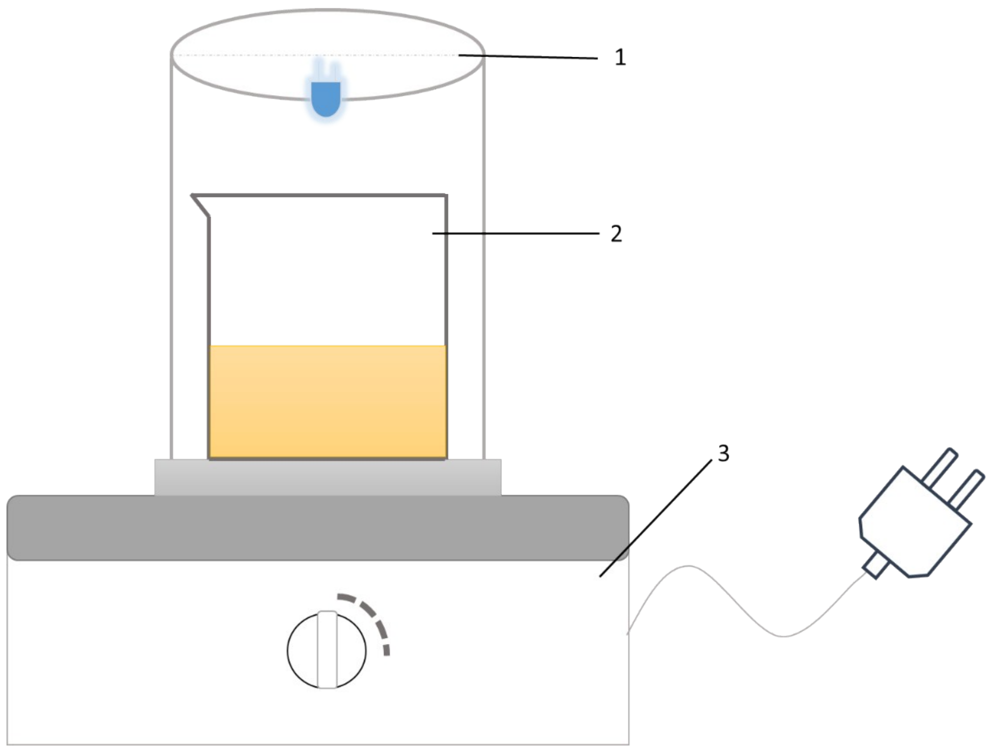

Fig. S2. Irradiation of the homemade photocatalytic reactor system: 1 = blue LED lamps, 2 = quartz breaker reaction vessel, 3 = magnetic stirrer

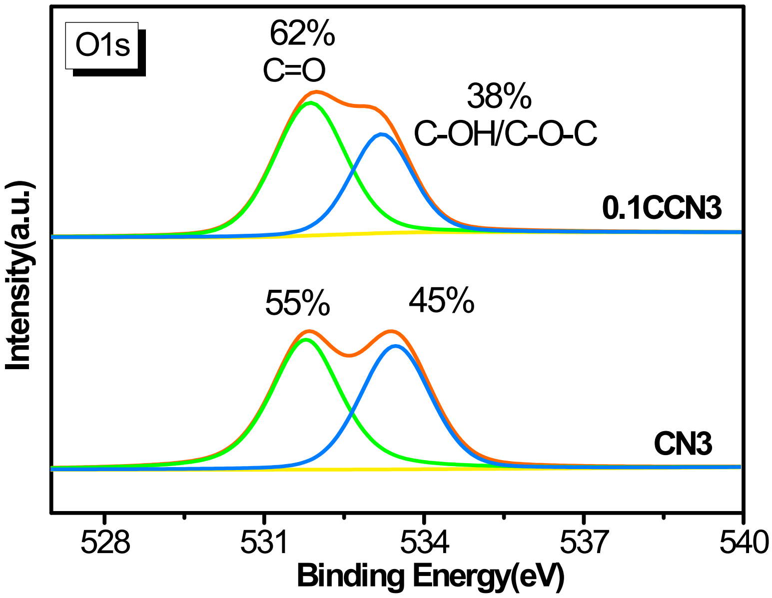

Fig. S3. XPS survey spectrum of CN3 and 0.1CCN3 and their corresponding high-resolution XPS spectrum of O1s regions.

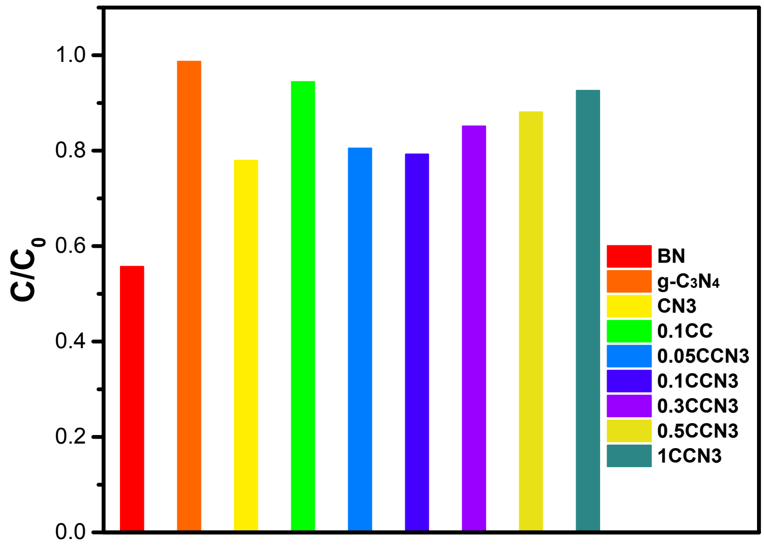

Fig. S4. The adsorption capacity of enrofloxacin over different photocatalysts before photoirradiation.

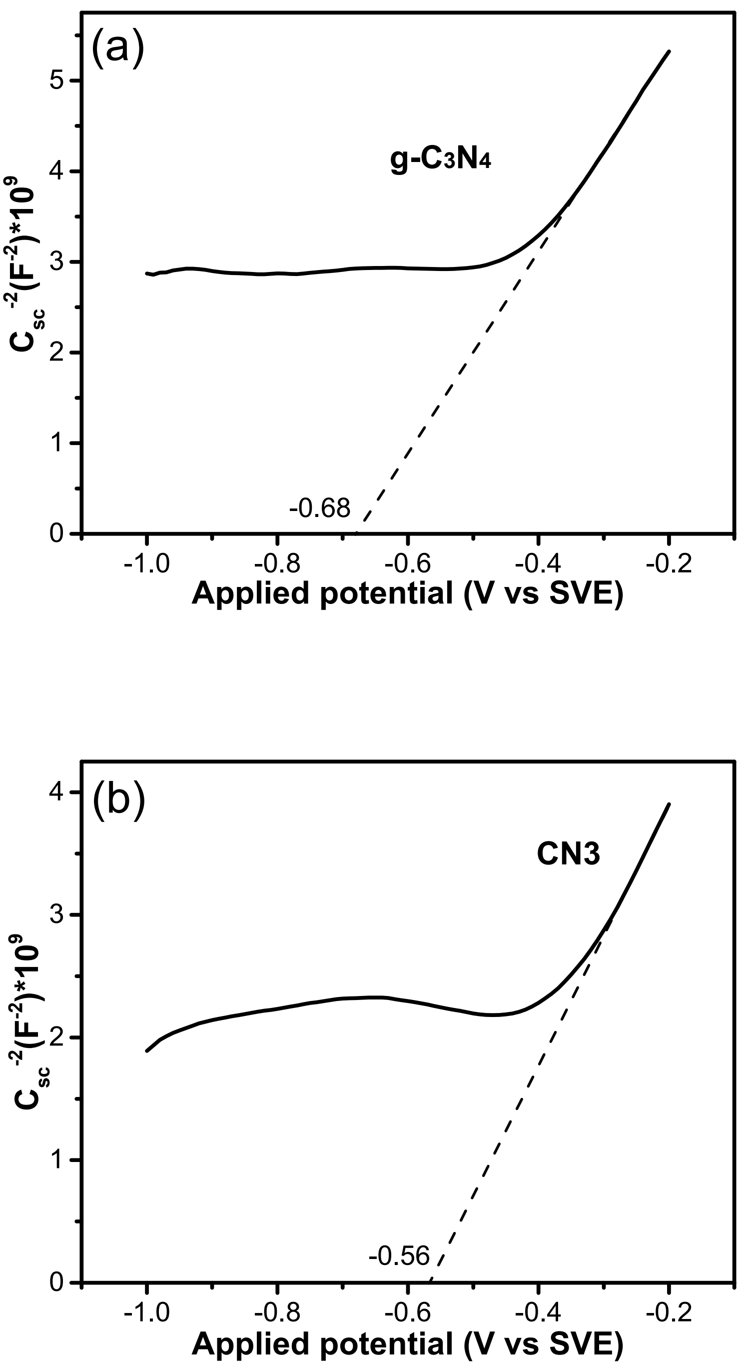
(a)
g-C3N4
-0.68
$C_{sc}^{-2}(F^{-2})*10^9$
Applied potential (V vs SVE)
(b)
CN3
-0.56
$C_{sc}^{-2}(F^{-2})*10^9$
Applied potential (V vs SVE)

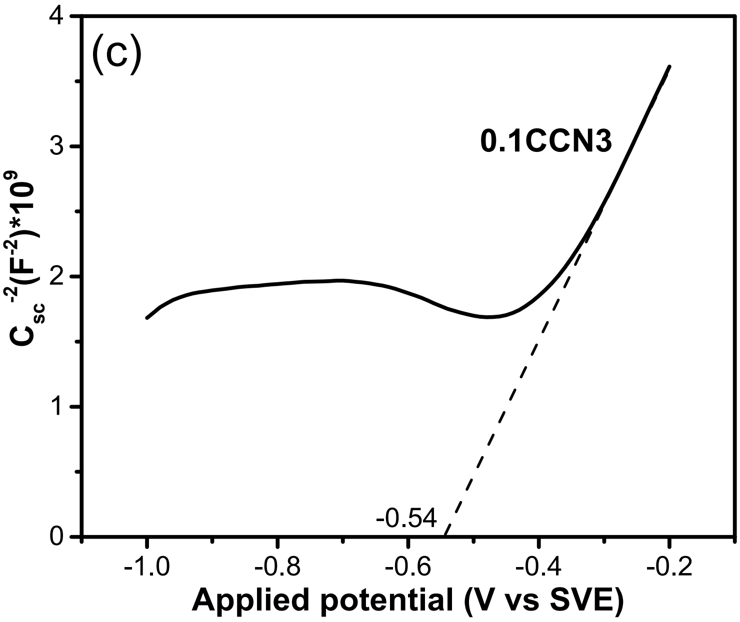

Fig. S5. Mott-Schottky plots for $g\text{-}C_3N_4$ (a), CN3 (b) and 0.1CCN3 (c).

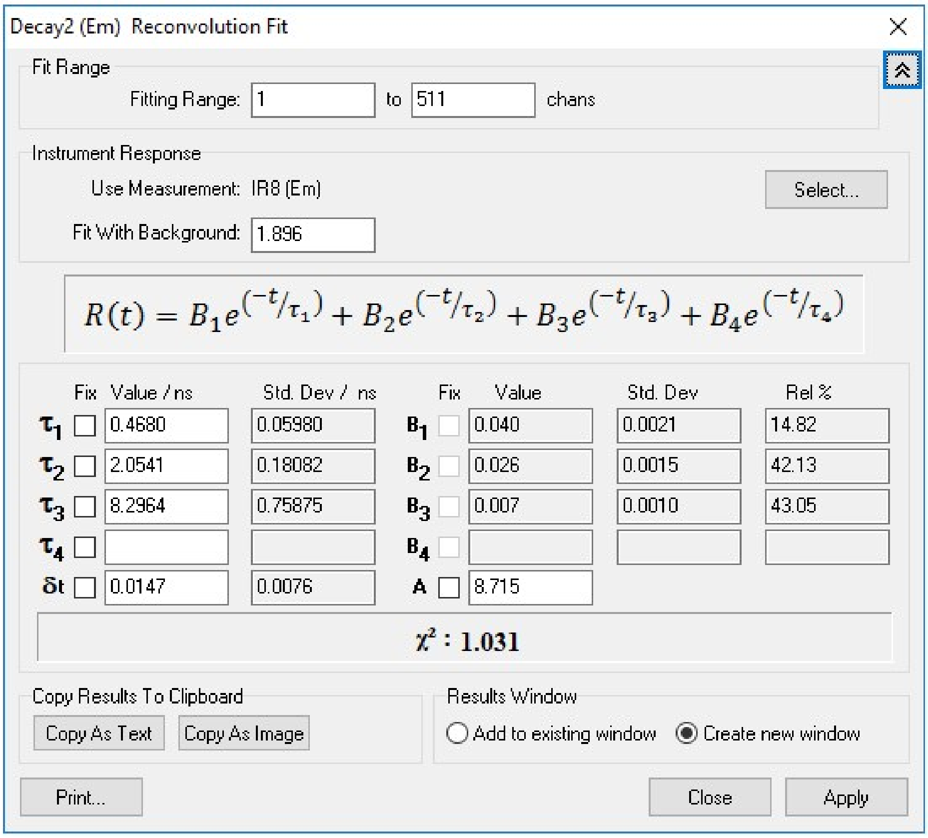

Fig. S6. Detailed fitting data of g-C_3N_4.

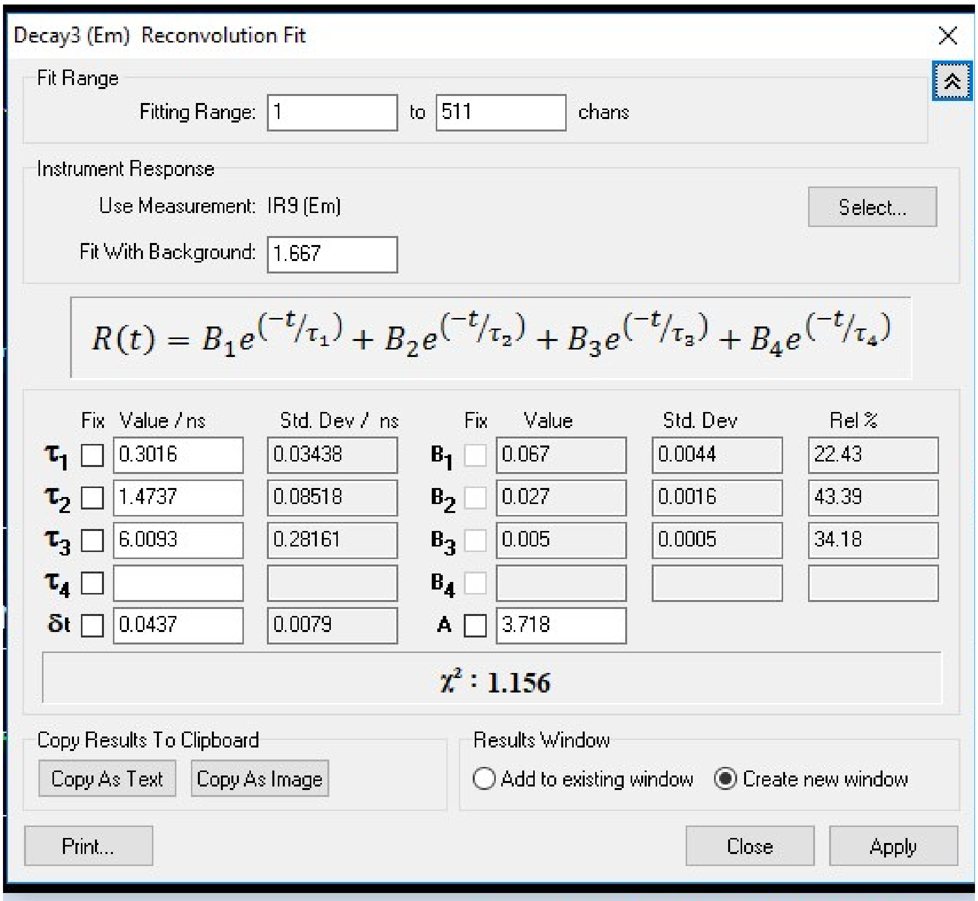

Fig. S7. Detailed fitting data of CN3.

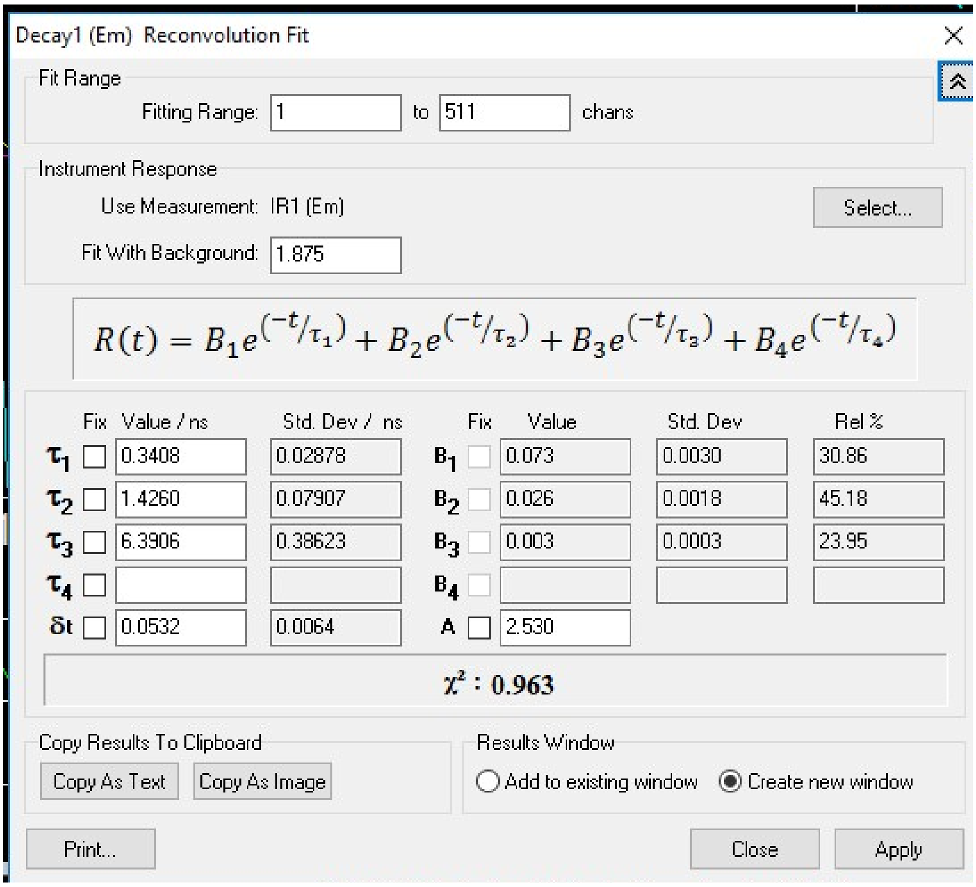

Fig. S8. Detailed fitting data of 0.1CCN3.